Blackbody-radiation shift in the Sr optical atomic clock

M. S. Safronova, S. G. Porsev, U. I. Safronova, M. G. Kozlov, and Charles W. Clark

Blackbody radiation shift in the Sr optical atomic clock

M. S. Safronova[1,2], S. G. Porsev[1,3], U. I. Safronova[4,5], M. G. Kozlov[3,6], and Charles W. Clark[2]

[1]*Department of Physics and Astronomy, University of Delaware, Newark, Delaware 19716, USA*
[2]*Joint Quantum Institute, National Institute of Standards and Technology and*
the University of Maryland, Gaithersburg, Maryland, 20899-8410, USA
[3]*Petersburg Nuclear Physics Institute, Gatchina, Leningrad District, 188300, Russia*
[4]*Physics Department, University of Nevada, Reno, Nevada 89557,*
[5]*Department of Physics, University of Notre Dame, Notre Dame, IN 46556*
[6]*St. Petersburg Electrotechnical University "LETI",*
Prof. Popov Str. 5, St. Petersburg, 197376, Russia

We evaluated the static and dynamic polarizabilities of the $5s^2$ $^1S_0$ and $5s5p$ $^3P_0^o$ states of Sr using the high-precision relativistic configuration interaction + all-order method. Our calculation explains the discrepancy between the recent experimental $5s^2$ $^1S_0 - 5s5p$ $^3P_0^o$ dc Stark shift measurement $\Delta\alpha = 247.379(7)$ [Middelmann *et al.*, arXiv:1208.2848 (2012)] and the earlier theoretical result of 261(4) a.u. [Porsev and Derevianko, Phys. Rev. A **74**, 020502R (2006)]. Our present value of 247.5 a.u. is in excellent agreement with the experimental result. We also evaluated the dynamic correction to the BBR shift with 1% uncertainty; -0.1492(16) Hz. The dynamic correction to the BBR shift is unusually large in the case of Sr (7%) and it enters significantly into the uncertainty budget of the Sr optical lattice clock. We suggest future experiments that could further reduce the present uncertainties.

I. INTRODUCTION

Optical lattice clocks have shown tremendous progress in recent years [1]. An optical frequency standard based on the $5s^2$ $^1S_0 - 5s5p$ $^3P_0^o$ transition of ultracold ^{87}Sr atoms confined in a one-dimensional optical lattice is pursued by a number of groups [2–8]. Its systematic uncertainty has been demonstrated at the 10^{-16} fractional frequency level and an order-of-magnitude improvement is expected to be achieved soon [1, 4]. A three-dimensional optical lattice clock with bosonic ^{88}Sr was demonstrated for the first time in [9].

The measured clock transition frequencies must be corrected in practice for the effect of the ambient blackbody radiation (BBR) shift, which is quite difficult to measure directly. The BBR shift can only be suppressed by cooling the clock. At room temperature, the differential BBR shift of the two levels of a clock transition turns out to make one of the largest irreducible contributions to the uncertainty budget of optical atomic clocks. The Sr clock transition has the largest BBR shift of all optical frequency standards that are currently under development (see Ref. [10] for a recent review). The fractional BBR shift $\Delta\nu_{\mathrm{BBR}}/\nu_0$ in Sr is more than a factor of 1000 larger than the fractional BBR shift in the Al$^+$ ion clock [11]. The BBR shift of an optical clock can generally be approximated by the dc Stark shift of the clock transition to about 1-2% precision, because optical frequencies are 100 times greater than characteristic BBR frequencies. However, Sr represents an exception, where the so-called dynamic correction [12], that needs to be determined separately from the dc Stark shift, is 7%.

Recently, the dc Stark shift in Sr has been measured

with 0.003% precision [13], and the dynamic correction was evaluated based on a set of $E1$ transition rates and the Stark shift measurement. The measured value differed substantially (by almost 4σ) from the previous theoretical determination [12].

In this work, we evaluate the static and dynamic polarizabilities of the $5s^2$ $^1S_0$ and $5s5p$ $^3P_0^o$ states of Sr using the high-precision relativistic CI+all-order method. Our calculation explains the above-mentioned discrepancy between the experimental $5s^2$ $^1S_0 - 5s5p$ $^3P_0^o$ dc Stark shift measurement $\Delta\alpha = 247.379(7)$ a.u. [13] and the earlier theoretical result of 261(4) a.u. [12]. We found that the $E1$ matrix elements for the transitions that give dominant contributions to the $^3P_0^o$ polarizability, in particular the $5s4d$ $^3D_1 - 5s5p$ $^3P_0^o$, are rather sensitive to the higher-order corrections to the wave functions and other corrections to the matrix elements beyond the random phase approximation. A correction of only 2.4% to the dominant $^3D_1 - {}^3P_0^o$ matrix element leads to 5% difference in the final value of the $^3P_0^o - {}^1S_0$ Stark shift. In this work, we included the higher-order corrections in an *ab initio* way using the CI+all-order approach, and also calculated several other corrections omitted in [12]. Our value for the dc Stark shift of the clock transition, 247.5 a.u., is in excellent agreement with the experimental result 247.379(7) a.u. [13].

We have combined our theoretical calculations with the experimental measurements of the Stark shift [13] and magic wavelength [3] of the $5s^2$ $^1S_0 - 5s5p$ $^3P_0^o$ transition to infer recommended values of the several electric-dipole matrix elements that give the dominant contributions to the $^3P_0^o$ polarizability. We used these values to evaluate the dynamic correction to the BBR shift of the $^1S_0 - {}^3P_0^o$

TABLE I: Comparison of experimental [14] and theoretical energy levels of Sr in cm^{-1}. Two-electron binding energies are given in the first row. The energies in other rows are given relative to the ground state. Results of the CI+MBPT and CI+all-order calculations are given in columns labeled "CI+MBPT" and "CI+All (A)". The CI+all-order values with the ground state two-electron binding energy shifted by 200 cm^{-1} are given in column labeled "CI+All (B)". Corresponding relative differences of these three calculations with experiment are given in the three corresponding columns labeled "Diff." in %. The $5s4d\ ^3D_1 - 5s5p\ ^3P_0^o$ transition energy is given in the last row.

State	Expt.	CI+MBPT	Diff.(%)	CI+All (A)	Diff.(%)	CI+All (B)	Diff.(%)
$5s^2\ ^1S_0$	134897	136244	1.00	135444	0.41	135244	0.26
$5s4d\ ^3D_1$	18159	18225	0.36	18327	0.93	18127	-0.18
$5s4d\ ^3D_2$	18219	18298	0.44	18394	0.96	18194	-0.13
$5s4d\ ^3D_3$	18319	18422	0.56	18506	1.02	18306	-0.07
$5s4d\ ^1D_2$	20150	20428	1.38	20441	1.45	20241	0.45
$5s6s\ ^3S_1$	29039	29369	1.14	29223	0.63	29023	-0.06
$5s6s\ ^1S_0$	30592	30938	1.13	30777	0.61	30577	-0.05
$5s5d\ ^1D_2$	34727	35092	1.05	34958	0.66	34758	0.09
$5s5d\ ^3D_1$	35007	35371	1.04	35210	0.58	35010	0.01
$5s5d\ ^3D_2$	35022	35388	1.04	35226	0.58	35026	0.01
$5s5d\ ^3D_3$	35045	35412	1.05	35250	0.59	35050	0.01
$5p^2\ ^3P_0$	35193	35854	1.88	35545	1.00	35345	0.43
$5p^2\ ^3P_1$	35400	36070	1.89	35758	1.01	35558	0.45
$5p^2\ ^3P_2$	35675	36344	1.88	36039	1.02	35839	0.46
$5s7s\ ^3S_1$	37425	37776	0.94	37606	0.48	37406	-0.05
$5s6d\ ^3D_1$	39686	40050	0.92	39876	0.48	39676	-0.02
$5s5p\ ^3P_0^o$	14318	14806	3.41	14550	1.62	14350	0.23
$5s5p\ ^3P_1^o$	14504	14995	3.38	14739	1.61	14539	0.24
$5s5p\ ^3P_2^o$	14899	15399	3.36	15142	1.63	14942	0.29
$5s5p\ ^1P_1^o$	21698	21955	1.18	21823	0.57	21623	-0.35
$4d5p\ ^3F_2^o$	33267	33719	1.36	33648	1.14	33448	0.54
$4d5p\ ^3F_3^o$	33590	34089	1.49	34003	1.23	33803	0.64
$4d5p\ ^3F_4^o$	33919	34444	1.55	34347	1.26	34147	0.67
$4d5p\ ^1D_2^o$	33827	34218	1.16	34208	1.13	34008	0.54
$5s6p\ ^3P_0^o$	33853	34241	1.15	34055	0.59	33855	0.00
$5s6p\ ^3P_1^o$	33868	34255	1.14	34071	0.60	33871	0.01
$5s6p\ ^3P_2^o$	33973	34365	1.15	34134	0.47	33934	-0.12
$5s6p\ ^1P_1^o$	34098	34476	1.11	34308	0.62	34108	0.03
$^3D_1 - ^3P_0^o$	3842	3419	-11.0	3777	-1.69	3777	-1.69

transition at 300 K to be -0.1492(16) Hz.

We determined that the $5s4d\ ^3D_1 - 5s5p\ ^3P_0^o$ transition contributed 98.2% to the dynamic correction for the $^3P_0^o$ level. Therefore, the uncertainty in the BBR shift can be further reduced by an accurate measurement of the lifetime of the $5s4d\ ^3D_1$ (or the term-averaged $5s4d\ ^3D$) state [15].

There is a correlation in the uncertainty of the BBR shift and the lifetime of the $5s4d\ ^3D_1$ state, if branching ratios are known to sufficient accuracy. At present, experimental measurements of the $5s4d\ ^3D$ term-averaged lifetime have an uncertainty of about 7% [16, 17]. We note that the experiment [16], which was performed at JILA some 20 years ago, has relevance in the determination of the uncertainty budget of one of the world's most accurate clocks now being developed at the same institution - a development probably not envisaged at the time.

A determination of $^3D_1$ (or ^3D) lifetime with 0.5% uncertainty would provide a value of the dynamic correction to the BBR shift of the clock $^1S_0 - ^3P_0$ transition at 300 K that is accurate to about 0.5%. The uncertainty in the dynamic correction dominates the uncertainty in the BBR shift at 300 K at the present time. Therefore, 0.5% improvement in the accuracy of the dynamic correction value will further reduce uncertainty in the BBR at 300 K by a factor of two. The extraction of the $5s4d\ ^3D_1 - 5s5p\ ^3P_0^o$ matrix elements from the lifetime measurement requires knowledge of the relevant branching ratios. We have determined these branching ratios with an uncertainty of 0.2%. A further reduction in the uncertainty of the Sr clock BBR shift could be effected by an improved measurement of these branching ratios. The lifetime of the corresponding $6s5d\ ^3D_1$ state in Yb has been recently measured in Ref. [15].

II. METHOD AND ENERGY LEVELS

Calculation of Sr properties requires an accurate all-order treatment of electron correlations. This can be

TABLE II: The CI+MBPT and CI+all-order results and further corrections to the $E1$ matrix elements for transitions that give dominant contributions to the polarizabilities of the $5s^2\,^1S_0$ and $5s5p\,^3P_0^o$ states. The CI+MBPT and CI+all-order results including RPA corrections are given in columns labeled "MBPT+RPA" and "All+RPA", respectively. The relative differences between the CI+all-order+RPA and CI+MBPT+RPA results are given in column labeled "Higher orders" in %. The other contributions include the core-Brueckner (σ), two-particle (2P), structural radiation (SR), and normalization (Norm) corrections. Total relative size of corrections beyond CI+all-order+RPA is given in column "Corr." in %. The recommended values for the $5s^2\,^1S_0 - 5s5p\,^1P_1^o$ matrix element was obtained from the $^1P_1^o$ lifetime measurement [18], and the recommended values for all other transitions are from the present work (see Section V).

Transition	MBPT+RPA	All+RPA	Higher orders	2P	σ	SR	Norm	Final	Corr.(%)	Recomm.
$5s^2\,^1S_0 - 5s5p\,^1P_1^o$	5.253	5.272	0.36%	−0.006	0.004	0.032	−0.094	5.208	−1.23	$5.248(2)^a$
$5s5p\,^3P_0^o - 5s4d\,^3D_1$	2.681	2.712	1.14%	−0.016	0.003	0.015	−0.048	2.667	−1.69	2.675(13)
$5s5p\,^3P_0^o - 5s6s\,^3S_1$	1.983	1.970	−0.66%	0.002	−0.001	−0.006	−0.025	1.940	−1.55	1.962(10)
$5s5p\,^3P_0^o - 5s5d\,^3D_1$	2.474	2.460	−0.57%	0.007	−0.001	−0.003	−0.031	2.432	−1.15	2.450(24)
$5s5p\,^3P_0^o - 5p^2\,^3P_1$	2.587	2.619	1.22%	0.009	0.003	0.021	−0.033	2.620	0.04	2.605(26)

^{a}Ref. [18];

accomplished within the framework of the CI+all-order method that combines configuration interaction and coupled-cluster approaches [11, 19–22]. To evaluate uncertainties of the final results, we also carry out CI [23] and CI+many-body perturbation theory (MBPT) [24] calculations. These methods have been described in a number of papers [11, 19, 23, 24] and we provide only a brief outline of these approaches.

We start with a solution of the Dirac-Fock (DF) equations

$$H_0\,\psi_c = \varepsilon_c\,\psi_c,$$

where H_0 is the relativistic DF Hamiltonian [19, 24] and ψ_c and ε_c are single-electron wave functions and energies. The calculations are carried out in the V^{N-2} potential. The wave functions and the low-lying energy levels are determined by solving the multiparticle relativistic equation for two valence electrons [23],

$$H_{\mathrm{eff}}(E_n)\Psi_n = E_n\Psi_n.$$

The effective Hamiltonian is defined as

$$H_{\mathrm{eff}}(E) = H_{\mathrm{FC}} + \Sigma(E),$$

where H_{FC} is the Hamiltonian in the frozen-core approximation. The energy-dependent operator $\Sigma(E)$ which takes into account virtual core excitations is constructed using second-order perturbation theory in the CI+MBPT method [24] and using a linearized coupled-cluster single-double method in the CI+all-order approach [19]. It is zero in a pure CI calculation. We refer the reader to Refs. [19, 24] for detailed description of the construction of the effective Hamiltonian.

Unless stated otherwise, we use atomic units (a.u.) for all matrix elements and polarizabilities throughout this paper: the numerical values of the elementary charge, $|e|$, the reduced Planck constant, $\hbar = h/2\pi$, and the electron mass, m_e, are set equal to 1. The atomic unit for polarizability can be converted to SI units via $\alpha/h\,[\mathrm{Hz}/(\mathrm{V/m})^2]{=}2.48832{\times}10^{-8}\alpha$ (a.u.), where the conversion coefficient is $4\pi\epsilon_0 a_0^3/h$ and the Planck constant

h is factored out in order to provide direct conversion into frequency units; a_0 is the Bohr radius and ϵ_0 is the electric constant.

As a first test of the accuracy of our calculations, we compare our theoretical energies with experiment for a number of the even- and odd-parity states. Comparison of the energy levels (in cm^{-1}) obtained in the CI+MBPT, and CI+all-order approximations with experimental values [14] is given in Table I. The ground state two-electron binding energies are given in the first row of Table I, energies in other rows are measured from the ground state. The relative differences of the CI+MBPT and CI+all-order calculations with experiment (in %) are given in columns labeled "Diff". Since the CI+all-order values are systematically higher than the experimental values, a large fraction of the difference from experiment can be attributed to the difference in the value of the ground state two-electron binding energy. We find that shifting the CI+all-order value of the ground state two-electron binding energy by only 200 cm^{-1} (see results in column CI+All (B)) brings the results into excellent agreement with experiment for most of the states. We give the $5s4d\,^3D_1 - 5s5p\,^3P_0^o$ transition energy in the last row of Table I. This transition is particulary important to the subject of this work, since it contributes 61% to the static polarizability and 98% to the dynamic correction of the BBR shift of the $5s5p\,^3P_0^o$ state. In fact, the accidentally small value of this transition energy is the source of the anomalously large (7%) dynamic correction to the BBR shift of the $^1S_0 - ^3P_0^o$ transition in Sr. We see considerable improvement of the calculation accuracy in this transition energy from the CI+MBPT to CI+all-order approximation, by a factor of 6. The CI+MBPT and CI+all-order values differ from the experiment by 11% and 1.7%, respectively.

TABLE III: Comparison of the electric dipole reduced matrix elements $|\langle\Psi||D_{\text{eff}}||\Psi'\rangle|$ (in a.u.) obtained in this work with other theoretical results (Porsev *et al.* [25] and Guo *et al.* [26]) and experimental measurements from [16–18, 27–31].

Transition	This work	Experiment	Theory [25]	Theory [26]
$5s5p\ ^3P_1^o - 5s^2\ ^1S_0$	0.158	0.151(2)[a]		0.13(1)
$5s5p\ ^1P_1^o - 5s^2\ ^1S_0$	5.272	5.248(2)[b]	5.28	5.15(15)
$5s6p\ ^1P_1^o - 5s^2\ ^1S_0$	0.281	0.26(2)[c]	0.236	
$4d5p\ ^1P_1^o - 5s^2\ ^1S_0$	0.517	0.60[c]		
$5s5p\ ^3P_0^o - 5s6s\ ^3S_1$	1.962(10)	2.03(6)[d]	1.96	1.90(1)
$5s5p\ ^3P_0^o - 5s7s\ ^3S_1$	0.516(8)	0.61(2)[e]	0.52	
$5s5p\ ^3P_0^o - 5p^2\ ^3P_1$	2.605(26)	2.5(1)[e]	2.56	
$5s5p\ ^3P_0^o - 5s4d\ ^3D_1$	2.675(13)	2.5(1)[f]	2.74	2.53(14)
		2.7(1)[g]		
$5s5p\ ^3P_0^o - 5s5d\ ^3D_1$	2.450(24)	2.3(1)[e]	2.50	
$5s5p\ ^3P_0^o - 5s6d\ ^3D_1$	1.161(17)		1.13	

[a]Ref. [30]; [b]Ref. [18]; [c]Ref. [27]; [d]Ref. [28]; [e]Ref. [29, 31]; [f]Ref. [16]; [g]Ref. [17].

III. *AB INITIO* CALCULATION OF ELECTRIC-DIPOLE MATRIX ELEMENTS

The reduced electric dipole matrix elements are obtained with the CI+all-order wave functions and effective electric-dipole operator D_{eff} in the random-phase approximation (RPA). The effective operator accounts for the core-valence correlations in analogy with the effective Hamiltonian [32, 33]. We include additional corrections beyond RPA in the calculation of the $E1$ matrix elements in comparison with [12, 25]. These contributions include the core-Brueckner (σ), two-particle (2P) corrections, structural radiation (SR), and normalization (Norm) corrections [32, 33]. While we find some cancelation between the various corrections, they cannot be omitted at the 1% level of accuracy. Partial cancelation of the structural radiation and normalization corrections was discussed in Ref. [34]. Detailed analysis of the structure radiation correction was carried out in the same work [34].

The results for several transitions that give dominant contributions to the $^1S_0 - {}^3P_0^o$ dc Stark shift are summarized in Table II. The percentage differences between the CI+all-order+RPA and CI+MBPT+RPA calculations are given in the column labeled "Higher orders". We note that it is positive for some transitions and negative for other transitions. Our final *ab initio* values are given in column labeled "Final". We find that total relative size of corrections beyond CI+all+RPA given in column labeled "Corr" is small, 0.04-1.7%, but significant. We estimate the uncertainties in the *ab initio* values of the matrix elements to be 1% based on the comparison of the CI+MBPT+RPA and CI+all-order+RPA values and combined size of other corrections.

In the present method, valence-valence correlations of two valence electrons are included via configuration interaction which is essentially complete for two electrons. Therefore, the dominant uncertainty arises from the core-valence correlations. The CI+all-order approach includes dominant core-valence higher-order (i.e. above second

order) corrections of this type. This has been tested in various other systems where precision data are available (see [15, 19, 35, 36] and references therein). Therefore, the size of dominant higher-order corrections may be estimated as the difference of the CI+all-order and CI+MBPT results. We assume that the size of the all other missing higher-order corrections does not exceed the size of the already included corrections. Therefore, the difference of the CI+all-order and CI+MBPT serves as an estimate of the uncertainty.

We also provide the recommended values for these transitions. The recommended value for the $5s^2\ ^1S_0 - 5s5p\ ^1P_1^o$ matrix element was obtained in [12, 25] from the $^1P_1^o$ lifetime measurement from photoassociation spectra [18]. The recommended values for all other transitions are obtained in the present work in Section V. Comparison of the final values of the electric dipole matrix elements with other theoretical results of Porsev *et al.* [25] and Guo *et al.* [26] and experimental measurements from [16–18, 27–31] is given in Table III. The theoretical results were obtained using the CI+MBPT method in Ref. [25] and CI method with semiempirical core polarization potential in Ref. [26]. The experimental values for the $5s5p\ ^3P_0^o - 5s4d\ ^3D_1$ matrix element were obtained from the ^3D term-averaged lifetimes measured in [16, 17] using our theoretical values of the branching ratios.

IV. POLARIZABILITIES

We evaluated the static and dynamic polarizabilities of the $5s^2\ ^1S_0$ and $5s5p\ ^3P_0^o$ states of Sr using the high-precision relativistic CI+all-order method. The scalar polarizability $\alpha_0(\omega)$ is separated into a valence polarizability $\alpha_0^v(\omega)$, ionic core polarizability α_c, and a small term α_{vc} that modifies ionic core polarizability due to the presence of two valence electrons. The valence part of the polarizability is determined by solving the inhomogeneous equation in valence space, which is approximated

TABLE IV: Contributions to the $5s^2\,^1S_0$ and $5s5p\,^3P_0^o$ static polarizabilities of Sr in a.u. The dominant contributions to the valence polarizabilities are listed separately with the corresponding absolute values of electric dipole reduced matrix elements given in columns labeled D. The theoretical and experimental [14] transition energies are given in columns ΔE_{th} and ΔE_{expt}. The remaining contributions to valence polarizability are given in rows Other. The contributions from the core and α_{vc} terms are listed together in rows Core + Vc. The dominant contributions to α_0, listed in columns $\alpha_0[A]$ and $\alpha_0(B)$, are calculated with CI + all-order +RPA (no other corrections) matrix elements and theoretical [A] and experimental [B] energies [14], respectively. The dominant contributions to α_0 listed in column $\alpha_0[C]$ are calculated with experimental energies and our final *ab initio* matrix elements. The dc Stark shift for the $5s5p\,^3P_0^o - 5s^2\,^1S_0$ transition is listed in the last rows of the table.

State	Contribution	ΔE_{th}	ΔE_{expt}	$D^{(a)}$	$\alpha_0[A]$	$\alpha_0[B]$	$D^{(b)}$	$\alpha_0[C]$
$5s^2\,^1S_0$	$5s^2\,^1S_0 - 5s5p\,^1P_1^o$	21823	21698	5.272	186.4	187.4	5.208	182.9
	$5s^2\,^1S_0 - 5s5p\,^3P_1^o$	14739	14504	0.158	0.25	0.25		0.25
	$5s^2\,^1S_0 - 5s6p\,^1P_1^o$	34308	34098	0.281	0.34	0.34		0.34
	$5s^2\,^1S_0 - 4d5p\,^1P_1^o$	41242	41172	0.517	0.95	0.95		0.95
	Other				4.60	4.60		4.60
	Core + Vc				5.29	5.29		5.29
	Total				197.8	198.9		194.4
	Recommended$^{(c)}$							197.14(20)
$5s5p\,^3P_0^o$	$5s5p\,^3P_0^o - 5s4d\,^3D_1$	3777	3842	2.712	285.0	280.2	2.667	270.9
	$5s5p\,^3P_0^o - 5s6s\,^3S_1$	14673	14721	1.970	38.7	38.6	1.940	37.4
	$5s5p\,^3P_0^o - 5s5d\,^3D_1$	20660	20689	2.460	42.9	42.8	2.432	41.8
	$5s5p\,^3P_0^o - 5p^2\,^3P_1$	21208	21083	2.619	47.3	47.6	2.620	47.6
	$5s5p\,^3P_0^o - 5s7s\,^3S_1$	23056	23107	0.516	1.69	1.69		1.69
	$5s5p\,^3P_0^o - 5s6d\,^3D_1$	25326	25368	1.161	7.8	7.8		7.8
	Other				29.1	29.1		29.1
	Core +Vc				5.55	5.55		5.55
	Total				458.1	453.4		441.9
	Recommended$^{(d)}$							444.51(20)
$^3P_0^o - {}^1S_0$					260.3	254.5		247.5
Theory [12]					261(4)			
Expt. [13]								247.379(7)

$^{(a)}$CI+all-order+RPA values (no other corrections). $^{(b)}$CI+all-order+RPA + other corrections. $^{(c)}$Obtained using experimental $5s5p\,^1P_1^o$ lifetime from [18]. $^{(d)}$Obtained using recommended value for the $^1S_0$ polarizability and the experimental value of the Stark shift [13].

as [37]

$$(E_v - H_{\text{eff}})|\Psi(v, M')\rangle = D_{\text{eff}}|\Psi_0(v, J, M)\rangle \qquad (1)$$

for the state v with total angular momentum J and projection M. The wave function $\Psi(v, M')$ is composed of parts that have angular momenta of $J' = J, J\pm 1$ that allows us to determine the scalar and tensor polarizabilities of the state $|v, J, M\rangle$ [37].

The core and α_{vc} terms are evaluated in the random-phase approximation. Their uncertainty is determined by comparing the DF and RPA values. The small α_{vc} term is calculated by adding α_{vc} contributions from the individual electrons, i.e. $\alpha_{vc}(5s^2) = 2\alpha_{vc}(5s)$, and $\alpha_{vc}(5s5p) = \alpha_{vc}(5s) + \alpha_{vc}(5p)$. The frequency dependence of the core and α_{vc} terms is negligible, and we use their static values in all calculations.

While we do not use the sum-over-states approach in the calculation of the polarizabilities, it is important to establish the dominant contributions to the final values. We combine the electric-dipole matrix elements and energies according to the sum-over-states formula for the

valence polarizability [38]:

$$\alpha_0^v(\omega) = \frac{2}{3(2J+1)} \sum_n \frac{(E_n - E_v)|\langle v\|D\|n\rangle|^2}{(E_n - E_v)^2 - \omega^2} \qquad (2)$$

to calculate the contributions of specific transitions. Here, J is the total angular momentum of the state v, D is the electric-dipole operator, E_i is the energy of the state i, and the frequency ω is zero in the static polarizability calculations.

We have carried out several calculations of the dominant contributions to the polarizabilities using different sets of the energies and $E1$ matrix elements in order to understand the difference of the theoretical predictions for the Stark shift $5s^2\,^1S_0 - 5s5p\,^3P_0^o$ $\Delta\alpha = 261(4)$ a.u. and recent experimental measurement $\Delta\alpha = 247.379(7)$ a.u. as well as to provide a recommended value for the $5s5p\,^3P_0^o - 5s4d\,^3D_1$ matrix element. The results are summarized in Table IV. Other theoretical calculations of Sr polarizabilities were recently compiled in review [38]. The ground-state polarizability of Sr was calculated using relativistic coupled-cluster (RCC) method in [39]. Their value 199.7(7.3) a.u. is in agreement with

our calculations.

In Table IV the absolute values of the corresponding reduced electric-dipole matrix elements are listed in columns labeled "D" in a.u.. The theoretical and experimental [14] transition energies are given in columns ΔE_{th} and ΔE_{expt}. The remaining valence contributions are given in rows labeled "Other". The contributions from the core and α_{vc} terms are listed together in row labeled "Core +Vc". The dominant contributions to α_0 listed in columns $\alpha_0[A]$ and $\alpha_0[B]$ are calculated with CI + all-order +RPA (no other corrections) matrix elements and theoretical [A] and experimental [B] energies [14], respectively.

Our $\alpha_0[A]$ result agrees with the earlier calculation of [12] which was carried out using CI+MBPT approach with energy fitting that approximated missing higher-order corrections to the wave functions. We note that this may be fortuitous since the calculation of [12] was carried out in V^N potential, while we are using V^{N-2} potential since the present version of the CI+all-order method is formulated for V^{N-2} potential. The E1 matrix elements in [12, 25] included RPA but omitted all other corrections calculated in the present work. We find that replacing the theoretical energies with experimental values reduces the Stark shift by 2.3%. We note that in the case of Sr all of the states contributing to the polarizabilities are included in our computational basis and this procedure is not expected to cause problems with basis set completeness, as in the case of Yb [40]. The dominant contributions to α_0 listed in column $\alpha_0[C]$ are calculated with experimental energies and final ab initio matrix elements. Inclusion of the small corrections further reduces the value of the Stark shift by 3.1%, and our resulting value obtained with our final *ab initio* matrix elements is in excellent agreement with experiment [13].

V. DETERMINATION OF RECOMMENDED VALUES OF ELECTRIC DIPOLE MATRIX ELEMENTS

We use three known experimental values: (i) the $5s5p\ ^1P_1^o$ lifetime [18], (ii) the Stark shift [13], and (iii) 814 nm magic wavelength [3] of the clock $^1S_0 - ^3P_0^o$ transition to improve the central values of the matrix elements and to reduce the uncertainties where possible.

Step 1. We use the $5s5p\ ^1P_1^o$ lifetime [18] to determine experimental value of the $5s^2\ ^1S_0 - 5s5p\ ^1P_1$ matrix element to be 5.248(2) a.u.

Step 2. The $5s^2\ ^1S_0 - 5s5p\ ^1P_1^o$ matrix element overwhelmingly dominates both ground state static and dynamic polarizability at 814 nm magic wavelength [3]. Therefore, we determine ground state static polarizability to be 197.14(20) a.u. and ac ground state polarizability at the magic wavelength to be 286.0(3) a.u.

Step 3. Now we have established two (mostly experimental) properties of the $5s5p\ ^3P_0^o$ state:

TABLE V: Breakdown of the contributions to the $5s5p\ ^3P_0^o$ static polarizability $\alpha_0(\omega = 0)$ and dynamic polarizability $\alpha_0(\omega)$ at the 813.4 nm magic wavelength. The dominant contributions to the valence polarizabilities are obtained with experimental energies and recommended values of the matrix elements. The electric-dipole reduced matrix elements are given in column labeled "D^{recom}". The experimental [14] transition energies are given in column labeled "ΔE_{expt}". The remaining contributions to valence polarizability are given in row labeled "Other". The contributions from the core and α_{vc} terms are listed together in row labeled "Core + Vc".

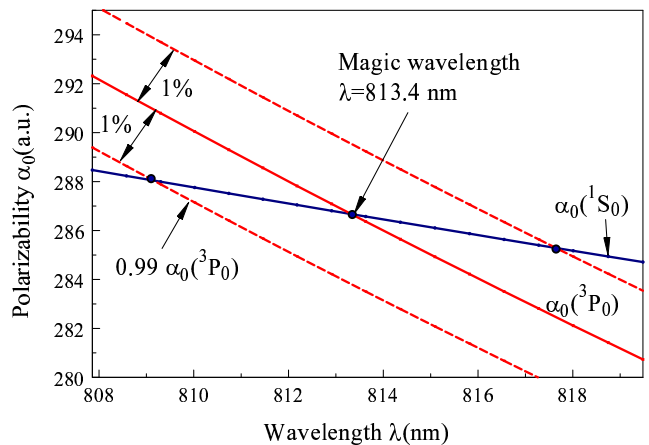| Contribution	ΔE_{expt}	D^{recom}	$\alpha_0(\omega)$	$\alpha_0(\omega = 0)$
$5s5p\ ^3P_0^o - 5s4d\ ^3D_1$	3842	2.675(13)	-29.5	272.6(3.3)
$5s5p\ ^3P_0^o - 5s6s\ ^3S_1$	14721	1.962(10)	126.4	38.3(4)
$5s5p\ ^3P_0^o - 5s5d\ ^3D_1$	20689	2.450(24)	65.6	42.5(8)
$5s5p\ ^3P_0^o - 5p^2\ ^3P_1$	21083	2.605(26)	71.4	47.1(9)
$5s5p\ ^3P_0^o - 5s7s\ ^3S_1$	23107	0.516(8)	2.4	1.69(5)
$5s5p\ ^3P_0^o - 5s6d\ ^3D_1$	25368	1.161(17)	10.2	7.8(2)
Other			34.1	29.1(9)
Core + Vc			5.55	5.55(6)
Total			286.0	444.5

FIG. 1: (Color online) The frequency-dependent polarizabilities of the Sr $5s^2\ ^1S_0$ and $5s5p\ ^3P_0^o$ states near 813.4 nm magic wavelength. The frequency-dependent polarizabilities of the $5s5p\ ^3P_0^o$ state shifted by $\pm$ 1% are shown to illustrate the sensitivity of the magic wavelength to this polarizability. The magic wavelength is marked with arrow.

(i) the static polarizability $\alpha(\omega = 0) = 444.5(2)$ a.u. is obtained by combining the experimental value of the $^1S_0 - ^3P_0^o$ Stark shift [13] with the $^1S_0$ polarizability above;

(ii) the ac polarizability at the magic wavelength $\alpha(\omega_{\text{magic}}) = 286.0(3)$ a.u.. This is because the ac polarizabilities of both $^1S_0$ and $^3P_0^o$ states are equal at this wavelength.

These two values are listed in the last row of Table V and serve as a basis for the determination of the recommended values and their uncertainties. Table V illustrates that different transitions give dominant contribu-

tions to static and dynamic polarizabilities.

Step 4. Three matrix elements give significant contributions to the $^3P_0^o$ ac polarizability at the magic wavelength (see column 4 of Table V): $5s5p$ $^3P_0^o - 5s6s$ $^3S_1$ (44%), $5s5p$ $^3P_0^o - 5s5d$ $^3D_1$ (23%), and $5s5p$ $^3P_0^o - 5p^2$ $^3P_1$ (25%). We start with all *ab initio* results and adjust values of these three matrix elements to obtain the total result of 286.0 a.u. The relative sizes of the adjustments in these transitions are based on the relative size and sign of the higher-order corrections and small contributions listed in Table II. We note that none of the changes exceeds 1.1%.

We plot the dynamic polarizabilities of the $^1S_0$ and $^3P_0^o$ states in the vicinity of the magic wavelength on Fig. 1 to illustrate that the crossing point is extremely sensitive to the matrix elements values. The 0.5% change in the values of the matrix elements (corresponding to 1% change in the value of the $^3P_0^o$ polarizability) shifts the crossing point by more than 4 nm. The magic wavelength is particularly sensitive to the value of the $5s5p$ $^3P_0^o - 5s6s$ $^3S_1$ matrix element, and we put its final uncertainty at 0.5%. We keep the uncertainties of the other two matrix elements at 1%.

Step 5. We now use these values to calculate the dc polarizability of the $^3P_0^o$ state. Then, we slightly (by 0.3%) adjust the *ab initio* value of the dominant $5s5p$ $^3P_0^o - 5s4d$ $^3D_1$ matrix element to get experimental result of 444.5 a.u (see last column of Table V). Then, very small adjustments are made to make sure that the final set of recommended values yields both static and dynamic polarizability values within their error bars.

We determine the uncertainty of the $5s5p$ $^3P_0^o - 5s4d$ $^3D_1$ matrix element from the uncertainty of all the other contributions to the $^3P_0^o$ polarizability value (listed in the last column of Table V). Since our theoretical values may experience a systematic shift in one direction, we add all of the uncertainties, totaling to 3.3 a.u, instead of adding them in quadrature. Assigning this value to be the uncertainty in the dominant $5s5p$ $^3P_0^o - 5s4d$ $^3D_1$ contribution of 272.7 a.u., we estimate the uncertainty in the recommended value of the corresponding matrix element to be 0.5%. Since the contributions to both static and dynamic polarizabilities from $5s5p$ $^3P_0^o - 5s7s$ $^3S_1$ and $5s5p$ $^3P_0^o - 5s6d$ $^3D_1$ transitions are small, we use *ab initio* CI+all+RPA values and assign them 1.5% uncertainty based on the size of the contributions listed in Table II.

VI. BLACKBODY RADIATION SHIFT

The leading contribution to the multipolar black body radiation (BBR) shift of the energy level g can be expressed in terms of the electric dipole transition matrix elements [41]

$$\Delta E_g = -\frac{(\alpha k_B T)^3}{2J_g + 1} \sum_n |\langle g||D||n\rangle|^2 F_1(y_n). \quad (3)$$

Here k_B is the Boltzmann constant, $y_n \equiv (E_n - E_g)/(k_B T)$, and $F_1(y)$ is the function introduced by Farley and Wing in [41]. Its asymptotic expansion is given by

$$F_1(y) \approx \frac{4\pi^3}{45y} + \frac{32\pi^5}{189y^3} + \frac{32\pi^7}{45y^5} + \frac{512\pi^9}{99y^7}. \quad (4)$$

The Eq. (3) can be expressed in terms of the dc polarizability $\alpha_g(\omega = 0)$ of the state g as [12]

$$\Delta E_g = -\frac{2}{15}(\alpha\pi)^3(k_B T)^4 \alpha_g(0) + \Delta E_g^{\mathrm{dyn}}. \quad (5)$$

Here $\Delta E_g^{\mathrm{dyn}}$ is determined as

$$\Delta E_g^{\mathrm{dyn}} \equiv -\frac{2}{15}(\alpha\pi)^3(k_B T)^4 \alpha_g(0)\eta \quad (6)$$

and η represents a "dynamic" fractional correction to the total shift that reflects the averaging of the frequency dependence of the polarizability over the frequency of the blackbody radiation spectrum. Corresponding shift in the clock transition frequency, $\Delta\nu_{^3P_0^o - ^1S_0}^{\mathrm{dyn}} = (\Delta E_{^3P_0^o}^{\mathrm{dyn}} - \Delta E_{^1S_0}^{\mathrm{dyn}})/h$, is referred to as dynamic correction to the BBR shift. The quantity η can be approximated by [12]

$$\eta = \eta_1 + \eta_2 + \eta_3 = \frac{80}{63(2J_g + 1)} \frac{\pi^2}{\alpha_g(0)k_B T}$$
$$\times \sum_n \frac{|\langle n||D||g\rangle|^2}{y_n^3} \left(1 + \frac{21\pi^2}{5 y_n^2} + \frac{336\pi^4}{11y_n^4}\right). \quad (7)$$

The dynamic corrections to the BBR shift of the $5s^2$ $^1S_0 - 5s5p$ $^3P_0^o$ clock transition in Sr at $T = 300$ K are given in Table VI (in Hz). The dynamic correction to the BBR shift of the $^3P_0^o$ level is dominated by the contribution from the $5s5p$ $^3P_0^o - 5s4d$ $^3D_1$ transition, which contributes 98.2% of the total. Our final result $-0.1492(16)$ Hz is in excellent agreement with recent value $-0.1477(23)$ Hz of Ref. [13].

Our result enables us to propose an approach for further reduction of the uncertainty in the BBR shift: a measurement of the $5s4d$ $^3D_1$ lifetime with 0.5% uncertainty would provide the value of the BBR shift in Sr clock that is accurate to about 0.5%, which would be a factor of 2 improvement in the uncertainty stated here. Such a determination assumes accurate knowledge of the branching ratios.

The $5s4d$ $^3D_1$ level decays to all three $5s5p$ $^3P_{0,1,2}^o$ states, but the branching ratio to the $^3P_2^o$ level is very small. The lifetime of a state a is calculated as

$$\tau_a = \frac{1}{\sum_{b \leq a} A_{ab}}.$$

The $E1$ transition rates A_{ab} are calculated using

$$A_{ab} = \frac{2.02613 \times 10^{18}}{\lambda^3} \frac{S}{2J_a + 1} \mathrm{s}^{-1},$$

TABLE VI: Dynamic corrections to the BBR shift of the $5s^2\ ^1S_0 - 5s5p\ ^3P_0^o$ clock transition in Sr at $T = 300\ K$ (in Hz). Quantities η_i, η, $\Delta E_g^{\mathrm{dyn}}$, and $\Delta\nu_{3P_0^o-{}^1S_0}^{\mathrm{dyn}}$ are defined in text.

	η_1	η_2	η_3	η	$\alpha_0(\omega=0)$	$\Delta E_g^{\mathrm{dyn}}/h$
Total $(5s^2\ ^1S_0)$	0.00163	0.00001	0	0.00164	197.1	-0.0028
$5s5p\ ^3P_0^o - 5s4d\ ^3D_1$	0.03394	0.00414	0.00088	0.03896		
$5s5p\ ^3P_0^o - 5s6s\ ^3S_1$	0.00032	0	0	0.00032		
$5s5p\ ^3P_0^o - 5s5d\ ^3D_1$	0.00018	0	0	0.00018		
$5s5p\ ^3P_0^o - 5p^2\ ^3P_1$	0.00019	0	0	0.00020		
$5s5p\ ^3P_0^o - 5s7s\ ^3S_1$	0.00001	0	0	0.00001		
$5s5p\ ^3P_0^o - 5s6d\ ^3D_1$	0.00002	0	0	0.00002		
Total $(5s5p\ ^3P_0^o)$	0.03467	0.00415	0.00088	0.03970	444.6	-0.1520
Final $\Delta\nu_{3P_0^o-{}^1S_0}^{\mathrm{dyn}}$						-0.1492(16)
Ref. [13]						-0.1477(23)

TABLE VII: Experimental transition energies (in cm^{-1}), theoretical line strengths (in a.u.), transition rates (in s^{-1}), and branching ratios for transitions contributing to the $5s4d\ ^3D_J$ lifetimes. The CI+RPA, CI+MBPT+RPA, and CI+all-order+RPA results are listed in columns labeled "CI", "MBPT", and "All", respectively. The recommended values of the $|\langle 5s5p\ ^3P_{1,2}^o||D_{\mathrm{eff}}||5s4d\ ^3D_{1,2}\rangle|$ and $|\langle 5s5p\ ^3P_2^o||D_{\mathrm{eff}}||5s4d\ ^3D_3\rangle|$ matrix elements are obtained using the recommended matrix element for the $5s4d\ ^3D_1 \rightarrow 5s5p\ ^3P_0^o$ transition (i.e. scaled by 0.9862). Experimental energies are used in all cases. Numbers in square brackets represent powers of 10.

Transition	ΔE_{epxt}	Line strengths S				Transition rates A_{ab}			Branching ratios		
		CI	MBPT	All	Recomm.	MBPT	All	Recomm.	CI	MBPT	All
$^3D_1 \rightarrow {}^3P_0^o$	3842	9.503	7.189	7.357	7.156	2.753[5]	2.817[5]	2.740[5]	0.5949	0.5954	0.5953
$^3D_1 \rightarrow {}^3P_1^o$	3655	7.172	5.414	5.543	5.391	1.785[5]	1.828[5]	1.777[5]	0.3866	0.3861	0.3862
$^3D_1 \rightarrow {}^3P_2^o$	3260	0.485	0.365	0.374	0.364	8.541[3]	8.750[3]	8.510[3]	0.0186	0.0185	0.0185
$\sum_{b\leq a} A_{ab}$						4.623[5]	4.722[5]	4.602[5]			
$^3D_2 \rightarrow {}^3P_1^o$	3714			16.605	16.149		3.448[5]	3.354[5]			0.8058
$^3D_2 \rightarrow {}^3P_2^o$	3320			5.602	5.449		0.831[5]	0.808[5]			0.1942
$\sum_{b\leq a} A_{ab}$							4.279[5]	4.162[5]			
$^3D_3 \rightarrow {}^3P_2^o$	3421			31.519	30.655		3.652[5]	3.552[5]			

where λ is the wavelength of the transition in $\mathring{A}$ and S is the line strength.

We find that the branching ratios are essentially independent of the correlation corrections to the matrix elements. We note that the line strength ratios are close to the non-relativistic ones (5/9, 5/12, 1/36), with the differences being -0.23%, $+0.22\%$, and 1.4% for the $^3D_1 - {}^3P_J^o$ transitions, respectively. We illustrate this point in Table VII, where we list the relevant energies, line strengths S, transition rates A, and branching ratios in the CI, CI+MBPT, and CI+all-order approximations.

We used the experimental energies in all calculations for consistency. We find that the difference in the CI, CI+MBPT, and CI+all-order branching ratio results is less than 0.1%. Since all the other corrections are small, their uncertainties should be even smaller. As a result, the accuracy of our branching ratios should be better than 0.2%. The recommended values for the $5s5p\ ^3P_{1,2}^o - 5s4d\ ^3D_1$ matrix elements are obtained using the recom-

TABLE VIII: The lifetimes of the $5s4d\ ^3D_J$ states in ns. The last three rows give term-averaged ^3D lifetime.

	MBPT	All	Recomm.
$\tau(5s4d\ ^3D_1)$	2163	2113	2171(24)
$\tau(5s4d\ ^3D_2)$		2337	2403(27)
$\tau(5s4d\ ^3D_3)$		2738	2816(31)
$\tau(5s4d\ ^3D)$		2453	2522(28)
Expt. [16]			2900(200)
Expt. [17]			2500(200)
Expt. [42]			4100(600)

mended matrix element for the $5s5p\ ^3P_0^o - 5s4d\ ^3D_1$ transition and CI+all-order branching ratios. The recommended values for the transition rates and the $5s4d\ ^3D_1$ lifetime, 2172(24) ns, are obtained using the recommended values of the matrix elements and experimental energies. We also list the recommended values $^3D_2$,

$^3D_3$, and term-averaged ^3D lifetimes in Table VIII. The ^3D term-averaged lifetime is compared with the experiments [16, 17, 42].

VII. CONCLUSION

We have evaluated the static and dynamic polarizabilities of the $5s^2\ ^1S_0$ and $5s5p\ ^3P_0^o$ states of Sr and explained the discrepancy between the recent experimental $5s^2\ ^1S_0 - 5s5p\ ^3P_0^o$ dc Stark shift measurement [13] and the earlier theoretical result [12]. Our theoretical value for the dc Stark shift of the clock transition, 247.5 a.u., is in excellent agreement with the experimental result. We have provided the recommended values of the matrix elements for transitions that give dominant contributions to the clock Stark shift and evaluated their uncertain-

ties. We evaluated the dynamic correction to the BBR shift of the $^1S_0 - \ ^3P_0^o$ clock transition at 300 K to be -0.1492(16) Hz and proposed an approach for further reduction of the uncertainty in the BBR shift.

[1] M. D. Swallows, M. J. Martin, M. Bishof, C. Benko, Y. Lin, S. Blatt, A. M. Rey, and J. Ye, IEEE Transactions on Ultrasonics, Ferroelectrics, and Frequency Control **59**, 416 (2012).

[2] G. K. Campbell, A. D. Ludlow, S. Blatt, J. W. Thomsen, M. J. Martin, M. H. G. de Miranda, T. Zelevinsky, M. M. Boyd, J. Ye, S. A. Diddams, et al., Metrologia **45**, 539 (2008).

[3] A. D. Ludlow, T. Zelevinsky, G. K. Campbell, S. Blatt, M. M. Boyd, M. H. G. de Miranda, M. J. Martin, J. W. Thomsen, S. M. Foreman, J. Ye, et al., Science **319**, 1805 (2008).

[4] S. Falke, H. Schnatz, J. S. R. Vellore Winfred, T. Middelmann, S. Vogt, S. Weyers, B. Lipphardt, G. Grosche, F. Riehle, U. Sterr, et al., Metrologia **48**, 399 (2011).

[5] X. Baillard, M. Fouché, R. Le Targat, P. G. Westergaard, A. Lecallier, F. Chapelet, M. Abgrall, G. D. Rovera, P. Laurent, P. Rosenbusch, et al., E. Phys. J. D **48**, 11 (2008).

[6] M. Takamoto, T. Takano, and H. Katori, Nature Photon. **5**, 288 (2011).

[7] E. A. Curtis, Y. B. Ovchinnikov, I. R. Hill, G. P. Barwood, and P. Gill, in *Frequency Standards and Metrology*, edited by L. Maleki (2009), pp. 218–222.

[8] A. Yamaguchi, N. Shiga, S. Nagano, Y. Li, H. Ishijima, H. Hachisu, M. Kumagai, and T. Ido, Appl. Phys. Express **5**, 022701 (2012).

[9] T. Akatsuka, M. Takamoto, and H. Katori, Nat. Phys. **4**, 954 (2008).

[10] M. S. Safronova, M. G. Kozlov, and C. W. Clark, IEEE Transactions on Ultrasonics, Ferroelectrics, and Frequency Control **59**, 439 (2012).

[11] M. S. Safronova, M. G. Kozlov, and C. W. Clark, Phys. Rev. Lett. **107**, 143006 (2011).

[12] S. G. Porsev and A. Derevianko, Phys. Rev. A **74**, 020502(R) (2006).

[13] T. Middelmann, S. Falke, C. Lisdat, and U. Sterr, Phys. Rev. Lett. **109**, 263004 (2012).

[14] Yu. Ralchenko, A. Kramida, J. Reader, and the NIST ASD Team (2011). NIST Atomic Spectra Database (version 4.1). Available at http://physics.nist.gov/asd. National Institute of Standards and Technology, Gaithersburg, MD.

[15] K. Beloy, J. A. Sherman, N. D. Lemke, N. Hinkley, C. W. Oates, and A. D. Ludlow, Phys. Rev. A **86**, 051404 (2012).

[16] D. A. Miller, L. Yu, J. Cooper, and A. Gallagher, Phys. Rev. A **46**, 062516 (1992).

[17] C. Redondo, M. Sanchezrayo, P. Ecija, D. Husain, and F. Castano, Chem. Phys. Lett. **392**, 116 (2004).

[18] M. Yasuda, T. Kishimoto, M. Takamoto, , and H. Katori, Phys. Rev. A **73**, 011403R (2006).

[19] M. S. Safronova, M. G. Kozlov, W. R. Johnson, and D. Jiang, Phys. Rev. A **80**, 012516 (2009).

[20] S. G. Porsev, M. S. Safronova, and M. G. Kozlov, Phys. Rev. Lett. **108**, 173001 (2012).

[21] M. S. Safronova, S. G. Porsev, M. G. Kozlov, and C. W. Clark, Phys. Rev. A **85**, 052506 (2012).

[22] M. S. Safronova, S. G. Porsev, and C. W. Clark, Physical Review Letters **109**, 230802 (2012), 1208.1456.

[23] S. A. Kotochigova and I. I. Tupitsyn, J. Phys. B **20**, 4759 (1987).

[24] V. A. Dzuba, V. V. Flambaum, and M. G. Kozlov, Phys. Rev. A **54**, 3948 (1996).

[25] S. G. Porsev, A. D. Ludlow, M. M. Boyd, and J. Ye, Phys. Rev. A **78**, 032508 (2008).

[26] K. Guo, G.-F. Wang, and A.-P. Ye, J. Phys. B **43**, 135004 (2010).

[27] W. H. Parkinson, E. M. Reeves, and F. S. Tomkins, J. Phys. B **9**, 157 (1976).

[28] G. Jönsson, C. Levinson, A. Persson, and C.-G. Wahlström, Z. Phys. A **316**, 255 (1984).

[29] G. Garca and J. Campos, J. Journal Quant, Spectr. Rad. Transfer **39**, 477 (1988).

[30] R. Drozdowski, M. Ignaciuk, J. Kwela, and J. Heldt, Z. Phys. D **41**, 125 (1997).

[31] J. E. Sansonetti and G. Nave, J. Phys. Chem. Ref. Data **39**, 033103 (2010).

[32] V. A. Dzuba, M. G. Kozlov, S. G. Porsev, and V. V. Flambaum, JETP **87**, 885 (1998).

[33] S. G. Porsev, Yu. G. Rakhlina, and M. G.Kozlov, Phys. Rev. A **60** 2781 (1999); J. Phys. B **32**, 1113 (1999).

[34] V. A. Dzuba, V. V. Flambaum, P. G. Silvestrov, and O. P. Sushkov, J. Phys. B **20**, 1399 (1987).

[35] M. S. Safronova, S. G. Porsev, M. G. Kozlov, and C. W. Clark, Phys. Rev. A **85**, 052506 (2012).

[36] M. S. Safronova, M. G. Kozlov, and U. I. Safronova, Phys. Rev. A **85**, 012507 (2012).

[37] M. G. Kozlov and S. G. Porsev, Eur. Phys. J. D **5**, 59 (1999).

[38] J. Mitroy, M. S. Safronova, and C. W. Clark, J. Phys. B **43**, 202001 (2010).

[39] B. K. Sahoo and B. P. Das, Phys. Rev. A **77**, 062516 (2008).

[40] V. A. Dzuba and A. Derevianko, J. Phys. B **43**, 074011 (2010).

[41] J. W. Farley and W. H. Wing, Phys. Rev. A **23**, 2397 (1981).

[42] E. N. Borisov, N. P. Penkin, and T. P. Redko, Opt. Spektrosk. **63**, 475 (1987).